Macromolecules
ARTICLE

Macromolecules **2010**, *43*, 6553–6561 **6553**
DOI: 10.1021/ma1009116

Two-Dimensional Bilayer Smectic Ordering of Rigid Rod−Rod Helical Diblock Polyisocyanides

Motonori Banno,[†] Zong-Quan Wu,[†] Kanji Nagai,[†] Shin-ichiro Sakurai,[‡] Kento Okoshi,[‡,§] and Eiji Yashima*[,†,‡]

[†]*Department of Molecular Design and Engineering, Graduate School of Engineering, Nagoya University, Chikusa-ku, Nagoya 464-8603, Japan, and* [‡]*Yashima Super-structured Helix Project, Exploratory Research for Advanced Technology (ERATO), Japan Science and Technology Agency (JST), Japan.* [§]*Present address: Department of Organic and Polymeric Materials, Graduate School of Engineering, Tokyo Institute of Technology, 2-12-1, Ookayama, Meguro-ku, Tokyo 152-8552, Japan.*

Received April 26, 2010; Revised Manuscript Received July 3, 2010

ABSTRACT: The rigid-rod-like left-handed helical polyisocyanides (poly-**3**) with a different molecular weight and a narrow molecular weight distribution were prepared by the living polymerization of an enantiomerically pure phenyl isocyanide bearing an L-alanine pendant with an *n*-hexyl chain (**3**) using the μ-ethynediyl Pt−Pd catalyst. The left-handed helical poly-**3**s maintain their living feature and further copolymerized an analogous L-alanine-bound phenyl isocyanide with a long *n*-tetradecyl chain (**4**) to produce rod−rod diblock polyisocyanides with a controlled helical sense and a narrow molecular weight distribution. The rigid rod−rod helical diblock copolyisocyanides were composed of the same L-alanine pendants, but with alkyl chains of different lengths self-assembled to form the nanometer-scaled bilayer smectic-like ordering on a substrate and in a liquid crystalline state as evidenced by the direct atomic force microscopic and polarized optical micrograph observations, respectively.

Introduction

Recently, supramolecular structures formed by macromolecular self-assembling building blocks such as rod−coil block copolymers have been studied extensively.[1] The rod segments are designed to possess a well-defined size and shape, so that the rod−coil block copolymers self-assemble to form unique three-dimensional (3D) architectures which include superlattices,[1b] superhelices,[1c] micelles,[1d] nanoribbons,[1e] and smectic liquid crystal (LC) phases.[1f] The morphology of these structures can be controlled by variation of the amphiphilicity, molecular weight, and the composition of the two components and solvents used as well. These findings have provided very useful knowledge and many prospects on the horizon leading to the discovery of novel self-assembling materials and the control of the dimensionality and shape of their structures through molecular design. These unique and specific properties may not be anticipated for most synthetic flexible polymers because of lack of the rigidity to retain unique 3D structures due to their totally random coil conformations.

Despite all these efforts, synthesis and self-assembling behaviors of rod−rod block copolymers have rarely been reported,[2] notwithstanding the many prospective applications in nanotechnology and scaffolds for the optoelectronic materials. Kros, Cornelissen, and co-workers designed a novel rod−rod amphiphile hybrid copolymers derived from helical poly(isocyanopeptide)s and poly(γ-benzyl L-glutamate) (PBLG) and found that they self-assembled into vesicles, "polymersome" in water.[3] The poly(isocyanopeptide)s have an enhanced rigidity of their helical backbones, resulting from a hydrogen-bonding network formed between the stacking amide groups of the peptide side chains,[1c,4] as observed in the α-helix of PBLG.[5] Similar amphiphilic rod−rod building blocks were also reported to form single-layer superstructures like vesicles, tubes, and sheets depending on their compositional periodicity.[6]

Previously, we reported that an enantiomerically pure phenyl isocyanide bearing an L-alanine pendant with a long *n*-decyl chain (**1**) was polymerized with the μ-ethynediyl Pt−Pd catalyst (**2**)[7] to produce both right (*P*)- and left (*M*)-handed helical, rigid-rod polyisocyanides at once with a different molecular weight (MW) and a narrow molecular weight distribution (MWD), which could be separated into each helix by facile fractionation with acetone.[8,9] The fractionated single-handed helical polyisocyanides maintained their living characteristics and can be used as an initiator (macroinitiator) for further block copolymerizations of the isocyanide enantiomers in a highly enantiomer-selective fashion along with an almost perfect helix-sense selectivity while retaining a narrow MWD (Figure 1A).[10] In addition, the rodlike macroinitiators and resulting block copolymers self-assembled to form a well-defined two-dimensional (2D) smectic ordering on the nanometer scale on a substrate; their molecular lengths and helical structures including the helical pitch, helical sense, and handedness excess could be directly determined by high-resolution atomic force microscopy (AFM) on a substate.[8,10]

Herein we show the synthesis and self-assembly behaviors of the rod−rod block helical polyisocyanides with a narrow MWD composed of enantiomerically pure phenyl isocyanide blocks bearing the same L-alanine residues with different alkyl chains, *n*-hexyl (**3**) and *n*-tetradecyl groups (**4**), as the pendants (Figure 1B). We anticipated that such rigid rod−rod helical block polyisocyanides consisting of anisotropically different cylindrical building blocks, resulting from short and long alkyl chains as the pendants instead of amphiphilicity, might dictate the self-assembly process and generate unique supramolecular architectures in order to minimize the steric hindrance between the neighboring building blocks. In addition, attractive van der Waals interactions between the pendant alkyl chains may also play a role for the self-assembly.

*To whom correspondence should be addressed. E-mail: yashima@apchem.nagoya-u.ac.jp.

Published on Web 07/23/2010

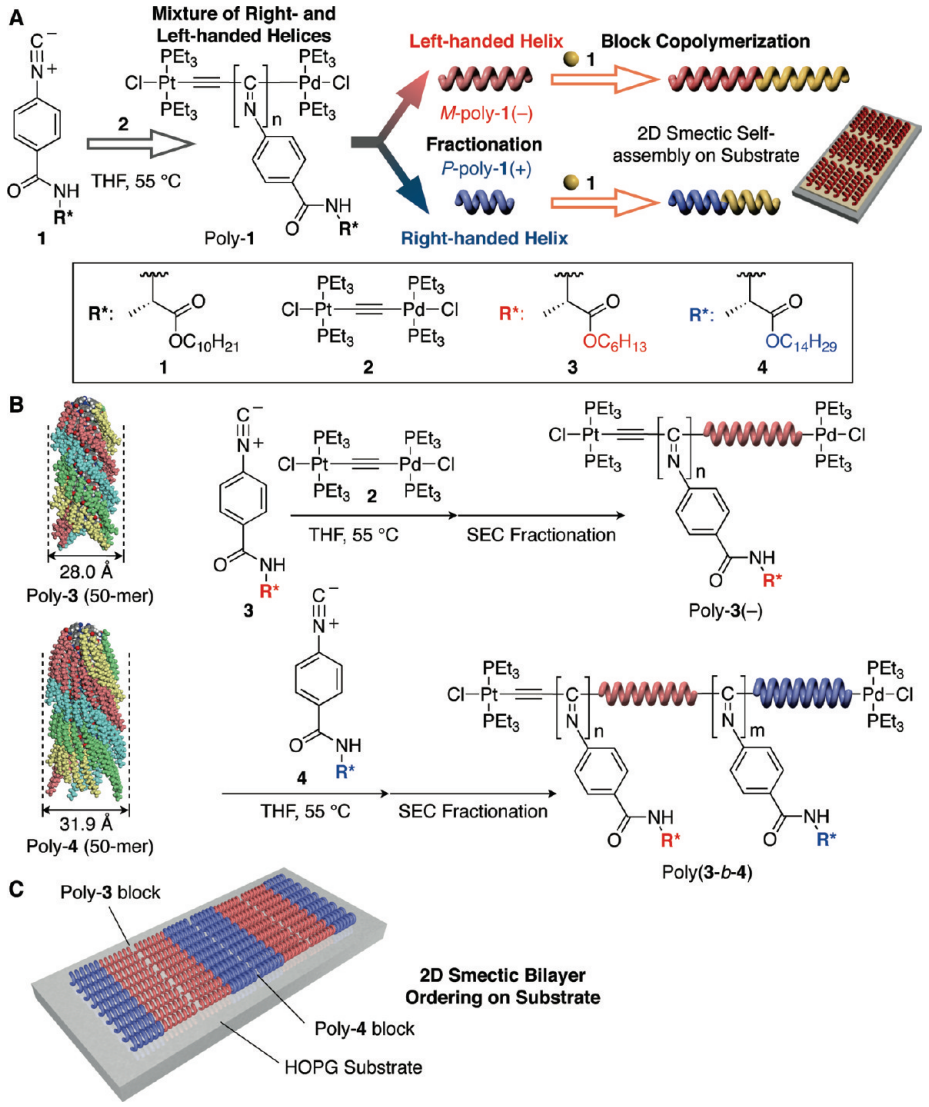

Figure 1. (A) Schematic illustration of the helix-sense-selective living polymerization of **1** with the μ-ethynediyl Pt−Pd catalyst (**2**), yielding a mixture of diastereomeric, right- and left-handed helical poly-**1**s with different MWs and a narrow MWD, which can be further separated into the right- and left-handed helical poly-**1**s. Each single-handed helical poly-**1** can be used as the macroinitiator for further block copolymerizations. The macroinitiators and resulting block copolymers self-assembled to form 2D smectic ordering on substrate.[8,10] (B) Synthesis and structures of poly(**3**-*b*-**4**)s with different block compositions. Possible helical structures of left-handed helical poly-**3** and poly-**4** on the basis of X-ray structural analyses of poly-**1**[8] followed by molecular mechanics calculation are also shown (left). Each structure is represented by space-filling models (50-mer). Four sets of helical arrays (n and $n + 4$) of the pendants are shown in different colors for clarity (red, yellow, green, and blue). (C) Schematic representation of 2D smectic head-to-head bilayer molecular ordering of poly(**3**-*b*-**4**) on a substrate. Red and blue colors represent poly-**3** and poly-**4** helical blocks, respectively.

Results and Discussion

A series of the block polyisocyanides (poly(**3**-*b*-**4**)s) with different **3** and **4** segment lengths were prepared according to the previously reported method[8,10] using the two-step living block polymerization of the isocyanide monomers (**3** and **4**) with the Pt−Pd catalyst (**2**) as outlined in Figure 1B. Poly-**3**s with different molecular weights (number-average molecular weight (M_n) = (2.95−6.09) × 10^4) and narrow MWDs (< 1.06) were first prepared by the polymerization of **3** with **2** as the initiator in tetrahydrofuran (THF) at 55 °C for 20 h. The obtained poly-**3**s contained minor right-handed helical poly-**3**s,[8,10] which could be separated off by size exclusion chromatography (SEC), thus producing the major almost complete left-handed helical poly-**3**s, as supported by their circular dichroism (CD) spectra (Figure 2) and SEC measurements (Figure 3). The obtained left-handed helical poly-**3**s[11] were used as macroinitiators for further block copolymerizations of **4** in THF at 55 °C to produce poly(**3**-*b*-**4**)s while maintaining a narrow MWD (Figure 3; see also Schemes 1 and 2). The CD spectral patterns and intensities of the block copolyisocyanides (Figure 2 and Table 1) in the imino chromophore regions of the polymer backbones (280—480 nm) as well as in the pendant aromatic regions (240—280 nm) are almost identical to those of the corresponding macroinitiators, clearly demonstrating that the present living block copolymerizations proceed in an almost perfect helix-sense-selective manner (Figure 2B).[10] The absolute M_n and degree of polymerization (DP) (see the suffixes of poly-**3**s and poly(**3**-*b*-**4**)s) of the macroinitiators and block copolymers were determined by SEC coupled with multi-angle light scattering (MALS) detector (SEC-MALS) measurements. The polymerization results are summarized in Table 1.

As expected from the rigid-rod-like features of the block copolymers with narrow MWDs, they exhibited smectic LC phases as evidenced by their clear fan-shaped textures in concentrated chloroform solutions under a polarized optical micrograph (Figure 4).[12]

Previously, we reported that the rodlike helical L-alanine-bound polyisocyanides with an *n*-decyl alkyl chain (poly-**1** in Figure 1A) as the pendant hierarchically self-assembled into smectic-like 2D

helix bundles (Figure 5A) on highly oriented pyrolytic graphite (HOPG) upon exposure to organic solvent vapors,[13] as revealed by AFM.[8,10] We then applied this procedure to visualize the 2D smectic structures of poly(**3**-*b*-**4**)s by measuring their AFM images.[15,16] Unlike rodlike helical polyisocyanide homopolymers, the rodlike helical copolymers, poly(**3**-*b*-**4**)s were composed of two different blocks with different cylindrical sizes while maintaining a narrow MWD and were anticipated to form a variety of 2D helix bundles with different geometries with respect to the molecular packing, head-to-head (H−H) or head-to-tail (H-T), parallel or antiparallel, and interdigitated or bilayer on a substrate. Such possible 2D helix-bundle structures are shown in Figure 5B−E.

Figure 6A shows the AFM images of poly($\mathbf{3}_{107}$-*b*-$\mathbf{4}_{92}$) deposited on HOPG from a dilute THF solution after THF vapor exposure at an ambient temperature for 12 h. The number-average molecular length (L_n) of the copolymer chains estimated by the AFM images was 17.0 nm (Figure 6C); this value is almost identical to that calculated by the SEC-MALS measurement results based on the absolute molecular weight and the unit height (0.087 nm) of a repeating unit of the analogous polyisocyanide[8] and nearly doubled in length compared to that of the macroinitiator poly-$\mathbf{3}_{107}$(−) (9.3 nm) (Table 1). Interestingly, a clear 2D smectic-like banded texture with periodicity was observed in the AFM image derived from the height variations of the segments composed of self-assembled block copolymer chains on HOPG. The brighter strata are higher than the darker strata by 0.2−0.3 nm in height, and the observed banding repeat distance estimated by the 2D fast Fourier transforms was ca. 37 nm (Figure 6B); the value is nearly twice as large as the length of poly($\mathbf{3}_{107}$-*b*-$\mathbf{4}_{92}$). The geometrical requirement can only be satisfied on the basis of the smectic H−H bilayer phase where a pair of smectic layers packs in a H−H fashion as illustrated in Figures 5B and 6D.

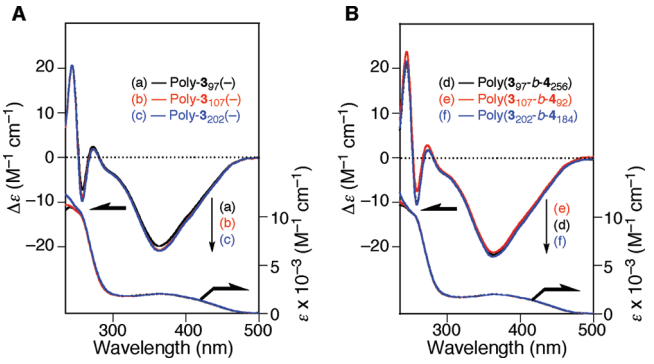

Figure 2. CD and absorption spectra of the macroinitiators and the resulting block copolymers measured in chloroform at 25 °C (0.2 mg/mL). (A) Macroinitiators: poly-$\mathbf{3}_{97}$(−) (a), poly-$\mathbf{3}_{107}$(−) (b), and poly-$\mathbf{3}_{202}$(−) (c). (B) Block copolymers: poly($\mathbf{3}_{97}$-*b*-$\mathbf{4}_{256}$) (d), poly($\mathbf{3}_{107}$-*b*-$\mathbf{4}_{92}$) (e), and poly($\mathbf{3}_{202}$-*b*-$\mathbf{4}_{184}$) (f).

In order to identify the high and low height strata of the banded textures to each block segment of the poly($\mathbf{3}_{107}$-*b*-$\mathbf{4}_{92}$), the AFM images of the corresponding 2D self-assembled homopolymers (poly-**3** and poly-**4**; DP = ca. 100) were measured (Figures 7 and 8, respectively). The average heights of each homopolymer were almost identical (ca. 1.7 nm), but a remarkable difference was observed in the chain-to-chain spacings of the self-assembled homopolymers on HOPG: ca. 2.0 nm for poly-**3** (Figure 7) and ca. 2.5 nm for poly-**4** (Figure 8). As described below, in-depth observations of the magnified AFM images of poly($\mathbf{3}_{107}$-*b*-$\mathbf{4}_{92}$) (Figure 9C) revealed that the chain-to-chain spacings were found to be larger (ca. 2.5−2.8 nm) for the dark segments than the bright ones (ca. 2.0 nm). On the basis of these observations, the segments in the poly($\mathbf{3}_{107}$-*b*-$\mathbf{4}_{92}$) with a higher height may be assigned to poly-**3** blocks and lower segments poly-**4** blocks, although the reason why the corresponding self-assembled homopolymers on HOPG had an almost identical height is not clear at the present.[17,18]

To visualize the exact ordering of poly($\mathbf{3}_{107}$-*b*-$\mathbf{4}_{92}$) molecules on HOPG, high-resolution AFM observations were performed. We could obtain well-defined smectic-like assemblies when the samples were prepared from a chloroform solution (Figure 9). In some areas, the smectic H−H bilayer molecular arrangements with junctures between the layers which appear to fit the molecular dimension of poly($\mathbf{3}_{107}$-*b*-$\mathbf{4}_{92}$) were clearly shown (see the zoomed images 1 and 2 in Figure 9C and schematic representations of a possible molecular ordering). In addition, there were also another types of ordering consisting of T−T interdigitated arrangements (for example, see the zoomed image 3 in Figure 9C) along with the major H−H bilayer arrangements. There were also the areas indicated by the circle in which the block copolymers did not form regular structures.

To further investigate the effect of the cylindrical segment lengths of poly(**3**-*b*-**4**)s on the formation of bilayer assemblies on HOPG, the AFM images of poly($\mathbf{3}_{97}$-*b*-$\mathbf{4}_{256}$) and poly($\mathbf{3}_{202}$-*b*-$\mathbf{4}_{184}$) with different lengths of poly-**3** and poly-**4** blocks (Table 1) were measured (Figures 10 and 11, respectively). Poly($\mathbf{3}_{97}$-*b*-$\mathbf{4}_{256}$) composed of shorter poly-**3** (8.5 nm) and longer poly-**4** blocks (ca. 22 nm) as schematically shown in Figure 10A also formed similar 2D helix bundles (Figure 10B), but in contrast to poly($\mathbf{3}_{107}$-*b*-$\mathbf{4}_{92}$), clear bilayer smectic-like banded textures derived from different height segments were hardly observed. This may be because the poly-**3** segments are too short compared to the poly-**4** ones to form a large domain to detect the difference in height by AFM. However, the magnified AFM image (Figure 10C) revealed that some segments could be assigned to the poly-**3** blocks because of a relatively shorter chain-to-chain spacing (2.0 nm) of the polymer ends, and the poly($\mathbf{3}_{97}$-*b*-$\mathbf{4}_{256}$) molecules seemed to pack in a complicated manner involving H−H bilayer, T−T interdigitated, and H−T arrangements as shown in Figure 10C.

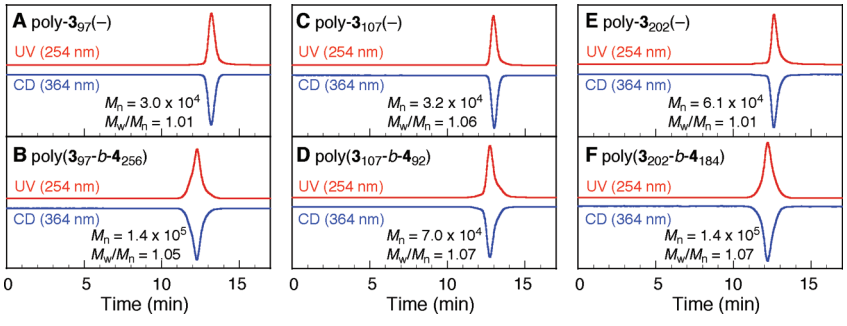

Figure 3. SEC chromatograms of the macroinitiators and block copolymers: poly-$\mathbf{3}_{97}$(−) (A), poly($\mathbf{3}_{97}$-*b*-$\mathbf{4}_{256}$) (B), poly-$\mathbf{3}_{107}$(−) (C), poly($\mathbf{3}_{107}$-*b*-$\mathbf{4}_{92}$) (D), poly-$\mathbf{3}_{202}$(−) (E), and poly($\mathbf{3}_{202}$-*b*-$\mathbf{4}_{184}$) (F) using UV (254 nm, red lines) and CD (364 nm, blue lines) detectors. The M_n and its distribution (M_w/M_n) of each polymer as determined by SEC-MALS measurements are also shown.

Scheme 1. Synthesis of Poly-3_{97}(−), Poly-3_{107}(−), and Poly-3_{202}(−)

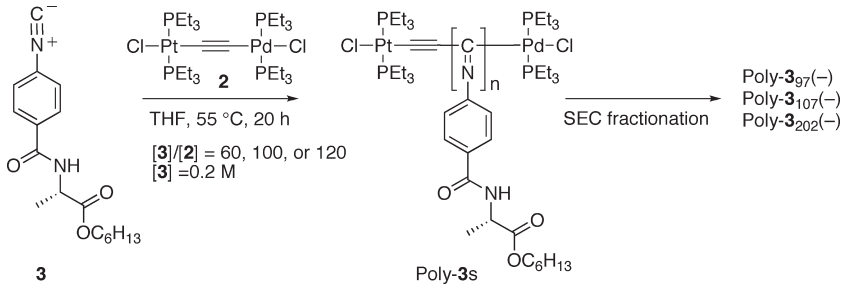

Scheme 2. Synthesis of Poly(3_{97}-*b*-4_{256}), Poly(3_{107}-*b*-4_{92}), and Poly(3_{202}-*b*-4_{184})

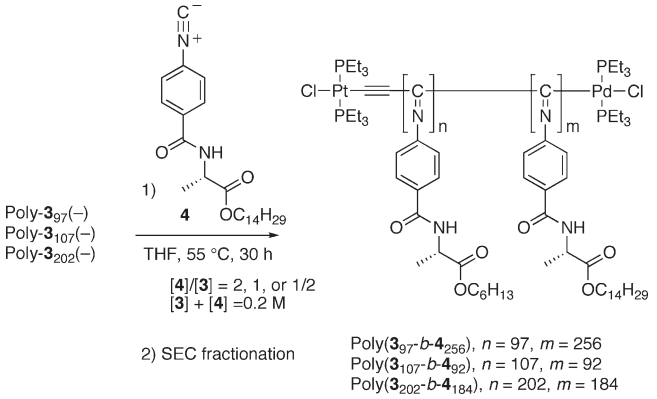

We tried to prepare a poly(**3**-*b*-**4**) copolymer consisting of longer poly-**3** and shorter poly-**4** blocks; however, only 55% of the macroinitiator (poly-3_{202}(−)) was found to react with **4** during the block copolymerization. As a result, the obtained copolymer poly(3_{202}-*b*-4_{184}) consisted of almost the same block length of poly-**3** and poly-**4** (Figure 11A), and the sample contained a small amount of the unreacted macroinitiator even after SEC fractionation because of the difficulty in separating it completely.[12]

The AFM images of poly(3_{202}-*b*-4_{184}) also showed 2D smectic-like bilayer structures with different height segments as observed in the banded textures of the poly(3_{107}-*b*-4_{92}) (Figure 11B). Again, the domains marked in red in the AFM image (right) can be assigned to the poly-**3** segments because of a relatively higher height and a shorter chain-to-chain spacing (2.0 nm). The observed periodic banding width of the poly-**3** was ca. 16 nm; this value is not twice as large as the block length of the poly-**3** in poly(3_{202}-*b*-4_{184}) unlike the case of poly(3_{107}-*b*-4_{92}). A possible explanation for this is the formation of a T−T interdigitated layer structure rather than the smectic H−H bilayer structure, as schematically depicted in Figure 5C, where the poly-**3** blocks are most likely interdigitated to each other to form such a bilayer structure. However, the high-resolution AFM image (Figure 11C) showed that the domain most likely consisted of ca. 20 poly-**4** blocks (blue lines) and 30 poly-**3** blocks (red lines), suggesting that the poly(3_{202}-*b*-4_{184}) may not form such a T−T interdigitated structure or the remaining poly-3_{202}(−) homopolymers may participate to form such a layer structure.

To eliminate the possibility that the macroinitiator could influence the formation of such a layer structure observed here, the high molecular weight part of the poly(3_{202}-*b*-4_{184}) was collected by further SEC fractionation to remove the macroinitiator completely, and then the AFM observations were performed again. The number-average molecular length of poly(3_{202}-*b*-4_{184}) after the SEC fractionation estimated by AFM images was 38.1 nm. The exact arrangements of the copolymers on HOPG could then be directly observed by high-resolution AFM, in which the poly-**3** and poly-**4** molecular segments were identified and marked in red and blue lines, respectively, on the basis of the differences in their heights and lateral spacings (Figure 12, right). The block copolymers packed in both H−H and H−T manners, and interdigitated overlapping of the poly-**3** segments also existed. There are unidentifiable segments and defects, and therefore, the full assignments of each copolymer chain including the two polymer ends and one juncture could not be perfectly attained. The difference in the molecular ordering of poly(3_{107}-*b*-4_{92}) and poly(3_{202}-*b*-4_{184}), consisting of almost the same ratio of poly-**3** and poly-**4** blocks, may be due to the difference in their molecular length. The smectic H−H ordering is not favored for such rodlike block copolymers with a long molecular length, since an effective packing becomes difficult in the 2D smectic H−H assemblies when the rods become longer.

In summary, we synthesized three different left-handed helical rod−rod diblock polyisocyanides with narrow MWDs composed of L-alanine-bound phenyl isocyanides bearing short *n*-hexyl and long *n*-tetradecyl chains as the pendants and provided the molecular arrangements of the diblock polyisocyanides in the 2D helix bundles on HOPG where each block segment was packed in the smectic-like arrangements, although the molecular arrangements were not perfectly controlled as revealed by the high-resolution AFM observations. The present AFM results at a molecular level clearly demonstrate that a small difference in the alkyl chain length at the pendant groups can be a major driving force for the constructing phase-separated nanomaterials on the substrates and will contribute to predict the 3D molecular ordering of rodlike helical polymers in liquid crystalline phases and in the solid state. We believe that the present methodology will be also useful for developing novel smectic liquid crystalline, rigid-rod block polyisocyanides composed of the desired monomer units with a controlled helicity through the living block copolymerization which may also provide unique chiral materials.

Experimental Section

Instruments. The NMR spectra were measured using a Varian AS500 spectrometer (Varian, Palo Alto, CA) operating at 500 MHz for ^{1}H and 125 MHz for ^{13}C using TMS as the internal standard. The IR spectra were recorded on a JASCO FT/IR-680 spectrometer (JASCO, Tokyo, Japan). The absorption and CD spectra were obtained in a 0.1 cm quartz cell at ambient temperature (20−25 °C) using a JASCO V570 spectrophotometer and a JASCO J820 spectropolarimeter, respectively. The polymer concentration was calculated on the basis of the monomer units and was 0.2 mg/mL. The optical rotations were measured in a 2 cm quartz cell on a JASCO P-1030 polarimeter. The SEC-MALS measurements were performed using an HLC-8220 GPC system (Tosoh, Tokyo, Japan) equipped with a differential refractometer coupled to a DAWN-EOS MALS device equipped with a semiconductor laser (λ = 690 nm) (Wyatt Technology, Santa Barbara, CA) operated at 25 °C using two TSKgel Multipore H_{XL}-M columns (Tosoh) in series, and THF containing 0.1 wt % tetra-*n*-butylammonium bromide

Table 1. Block Copolymerization Results of 4 Initiated by Poly-3 in THF at 55 °C

				molecular weight[a]		molecular length (nm)			
run	polyisocyanide	time (h)	yield (%)	M_n ($\times 10^{-4}$)	M_w/M_n	L_n(calc)[b]	L_n(obs)[c]	L_w/L_n[c]	$\Delta\varepsilon_{364}$[d] (M^{-1} cm^{-1})
1	poly-$\mathbf{3}_{97}$(−)	20	92 (70)[e]	2.95	1.01	8.5	—[f]	—[f]	−20.0
2	poly-$\mathbf{3}_{107}$(−)	20	94 (56)[e]	3.23	1.06	9.3	—[f]	—[f]	−21.0
3	poly-$\mathbf{3}_{202}$(−)	20	99 (76)[e]	6.09	1.01	17.5	20.3	1.06	−21.0
4	poly($\mathbf{3}_{97}$-*b*-$\mathbf{4}_{256}$)	30	78 (70)[e]	13.6	1.05	30.7	31.0	1.27	−21.0
5	poly($\mathbf{3}_{107}$-*b*-$\mathbf{4}_{92}$)	30	100 (80)[e]	7.02	1.07	17.3	17.0	1.10	−21.0
6	poly($\mathbf{3}_{202}$-*b*-$\mathbf{4}_{184}$)	30	55 (75)[e]	13.7	1.07	33.5	34.0	1.22	−20.0

[a] Determined by SEC-MALS measurements with THF containing TBAB (0.1 wt %) as the eluent. [b] Calculated by the M_n values based on the molecular weights of the monomers (302.4 for **3** and 414.6 for **4**) and the unit height (0.087 nm) of a repeating unit of polyisocyanides determined by X-ray diffraction (XRD) analysis of an analogous L-alanine-bound helical polyisocyanide (poly-**1**).[8] [c] Estimated by AFM measurements based on an evaluation of ca. 500 molecules. [d] Measured in chloroform at 25 °C. [e] The yield after SEC fractionation is shown in the parentheses. [f] Not determined.

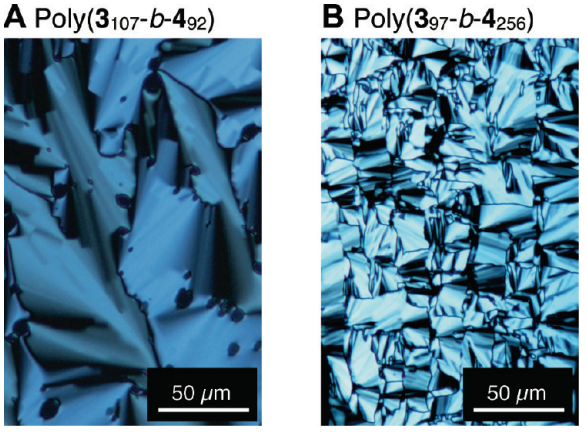

Figure 4. Polarized optical micrographs of poly($\mathbf{3}_{107}$-*b*-$\mathbf{4}_{92}$) (A) and poly($\mathbf{3}_{97}$-*b*-$\mathbf{4}_{256}$) (B) in chloroform solution taken at ambient temperature. Clear fan-shaped textures typical of smectic phases were observed.

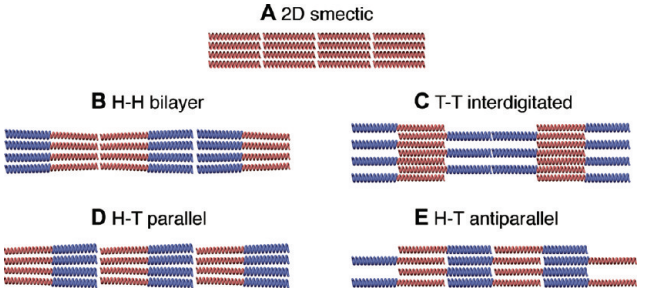

Figure 5. Schematic representation of the 2D smectic ordering of homopolymer (A) and typical 2D helix-bundle structures of diblock copolymers with different geometries with respect to the molecular packing (B−E); head-to-head bilayer (B), tail-to-tail interdigitated (C), head-to-tail parallel (D), and head-to-tail antiparallel (E).

(TBAB) was used as the eluent at the flow rate of 0.5 mL/min. The scattered light intensities were measured by 18 light scattering detectors at different angles. The differential refractive index increment, dn/dc, of the polymer with respect to the mobile phase at 25 °C was also measured by an Optilab rEX interferometric refractometer (Wyatt Technology). SEC fractionation of the polymers (poly-$\mathbf{3}_{97}$, poly-$\mathbf{3}_{107}$, poly-$\mathbf{3}_{202}$, poly($\mathbf{3}_{97}$-*b*-$\mathbf{4}_{256}$), poly($\mathbf{3}_{107}$-*b*-$\mathbf{4}_{92}$), and poly($\mathbf{3}_{202}$-*b*-$\mathbf{4}_{184}$)) was carried out using a JASCO PU-2080 Plus liquid chromatograph equipped with UV−vis (JASCO UV-2070Plus) and RI (RI-2031Plus) detectors with two G4000HHR columns (Tosoh) connected in series. THF containing 0.1 wt % TBAB was used as the eluent at the flow rate of 5.0 mL/min. The AFM measurements were performed using a Nanoscope IIIa or Nanoscope IV microscope (Veeco Instruments, Santa Barbara, CA) in air at ambient temperature (ca. 25 °C) with standard silicon cantilevers (NCH, NanoWorld, Neuchâtel, Switzerland) in the tapping mode. The polarizing optical microscopic observations

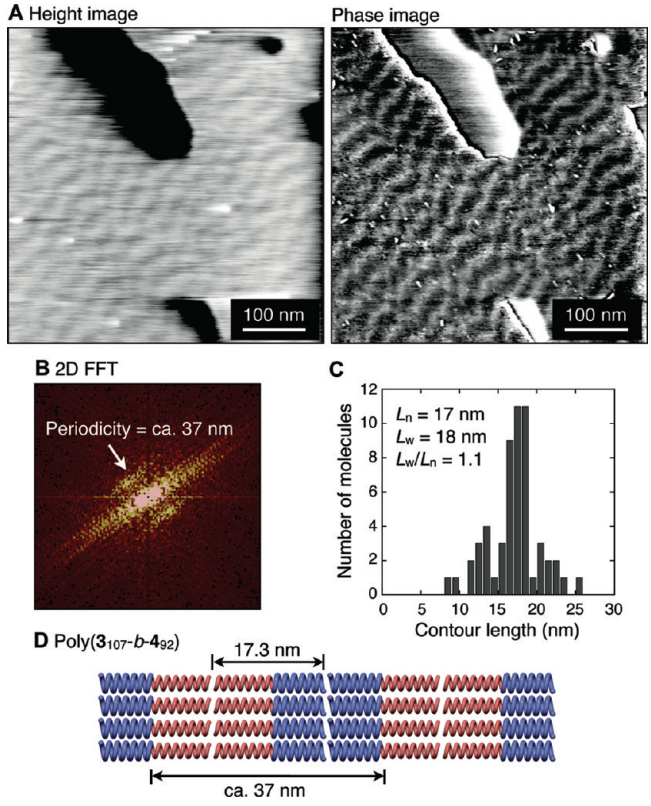

Figure 6. (A) AFM height (left) and phase (right) images of 2D self-assembled poly($\mathbf{3}_{107}$-*b*-$\mathbf{4}_{92}$) on HOPG. The samples were prepared by depositing a dilute THF solution (0.02 mg/mL), followed by exposure to THF vapor for 12 h at ambient temperature (ca. 25 °C). The 2D fast Fourier transform of the phase image indicating the periodicity of ca. 37 nm is also shown in (B). (C) Histogram of the length distribution of poly($\mathbf{3}_{107}$-*b*-$\mathbf{4}_{92}$) obtained from high-resolution AFM images. The number-average length (L_n), the weight-average length (L_w), and the length distribution (L_w/L_n) were estimated on the basis of the evaluation of more than 100 molecules. (D) Schematic representation of the 2D smectic H−H bilayer molecular ordering of poly($\mathbf{3}_{107}$-*b*-$\mathbf{4}_{92}$) on HOPG. Poly-**3** and poly-**4** blocks are indicated by red and blue colors, respectively.

were carried out with an E600POL polarizing optical microscope (Nikon, Tokyo, Japan) equipped with a DS-5 M CCD camera (Nikon) connected to a DS-L1 control unit (Nikon). The sample solution was placed on a glass plate with a cover glass to develop the planar structure before observation of the microscopic texture at ambient temperature (20−25 °C).

Materials. Anhydrous THF and chloroform (water content < 50 ppm) were purchased from Wako (Osaka, Japan) and stored under dry nitrogen. THF was further dried over sodium benzophenone ketyl, distilled onto $LiAlH_4$ under nitrogen, and distilled under high vacuum just before use. The 4-isocyanobenzoyl-L-alanine hexyl ester (**3**) and 4-isocyanobenzoyl-L-alanine

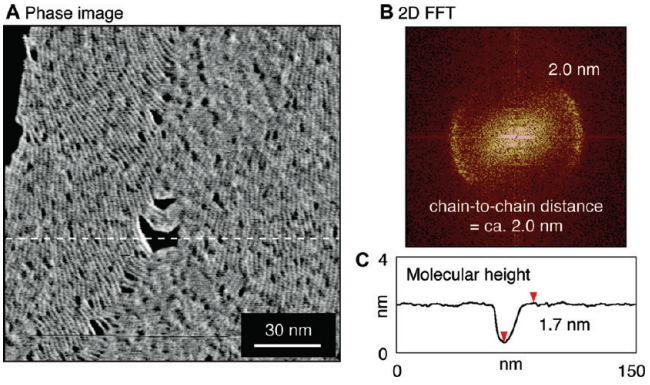

Figure 7. (A) AFM phase image of 2D self-assembled poly-**3** on HOPG and (B) typical 2D fast Fourier transform of (A), indicating the chain-to-chain distance of 2.0 nm. The cross-sectional profile denoted by the white dashed line is also shown in (C).

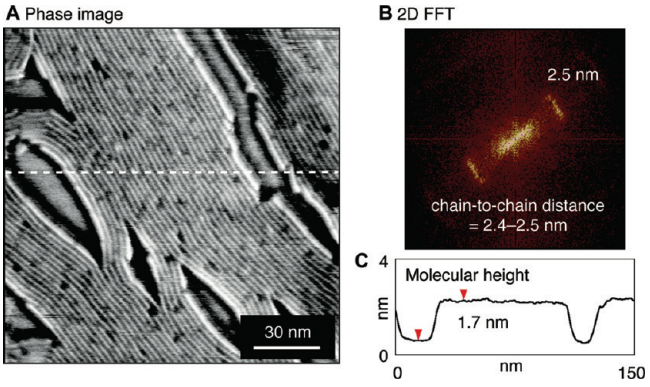

Figure 8. (A) AFM phase image of 2D self-assembled poly-**4** on HOPG and (B) typical 2D fast Fourier transform of (A), indicating the chain-to-chain distance of 2.4−2.5 nm. The cross-sectional profile denoted by the white dashed line is also shown in (C).

tetradecyl ester (**4**)[9b] were prepared as previously reported. The μ-ethynediyl Pt−Pd catalyst (**2**)[7] was a gift from Prof. Onitsuka of Osaka University.

Polymerization. The polymerization of **3** was carried out in a dry glass ampule under a dry nitrogen atmosphere using **2** as the initiator in dry THF in a similar way to that previously reported.[8] A typical experimental procedure is described below (Scheme 1). Monomer **3** (100 mg, 0.33 mmol) was placed in a dry ampule, which was then evacuated on a vacuum line and flushed with dry nitrogen. After this evacuation−flush procedure had been repeated three times, a three-way stopcock was attached to the ampule, and dry THF (1.41 mL) was added by a syringe. To this was added a solution of **2** in THF (13.8 mM, 0.24 mL) at ambient temperature. The concentrations of **3** and **2** were 0.2 and 0.002 M, respectively ([**3**]/[**2**] = 100). The mixture was then stirred under a dry nitrogen atmosphere and heated to 55 °C. After 20 h, the resulting polymer (poly-**3**) was precipitated in a large amount of methanol, collected by centrifugation, and dried *in vacuo* at room temperature overnight (96.8 mg, 94% yield).

In the same way, poly-**3**s with different molecular weights ([**3**]/[**2**] = 60 and 120) were prepared by the polymerization of **3** with **2** in THF at 55 °C for 20 h.

Preparation of Single-Handed Helical Poly(phenyl isocyanide) Macroinitiators. The obtained poly-**3**s were found to contain a small amount of right-handed helical poly-**3**s with a lower molecular weight as reported previously,[8] as evidenced by a bimodal SEC distribution with a sharp main peak together with a small peak in the lower molecular weight region whose CD signs were opposite, negative (left-handed) and positive (right-handed), respectively (Figure S2).[8] We then purified and isolated the major left-handed helical poly-**3**s by SEC fractionation using THF containing 0.1 wt % TBAB as the eluent. A typical

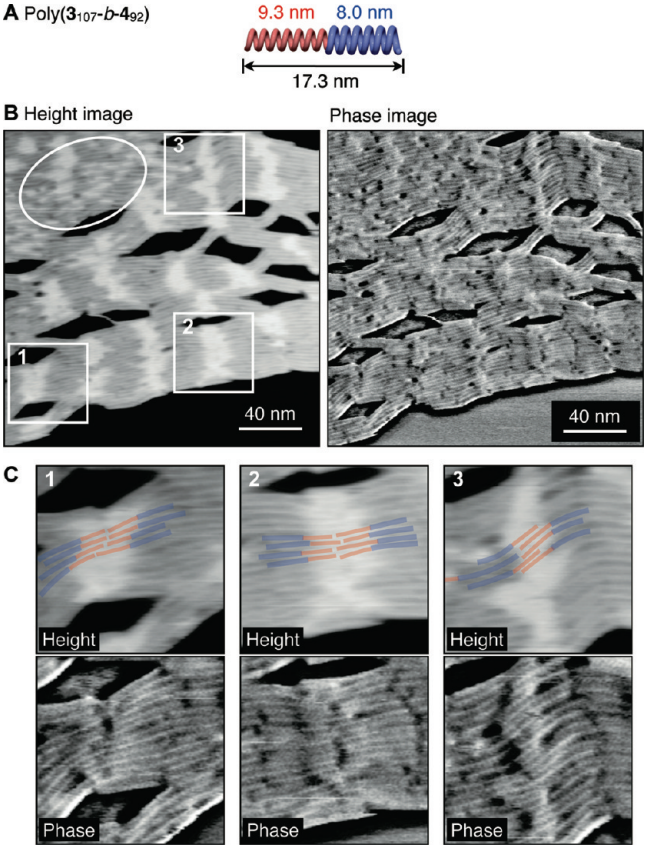

Figure 9. (A) Schematic structure of poly($\mathbf{3}_{107}$-*b*-$\mathbf{4}_{92}$) and (B) high-resolution AFM height (left) and phase (right) images of 2D self-assembled poly($\mathbf{3}_{107}$-*b*-$\mathbf{4}_{92}$) on HOPG. The samples were prepared by depositing a dilute chloroform solution (0.02 mg/mL), followed by exposure to chloroform vapor for 12 h at ambient temperature (ca. 25 °C). (C) Zoomed height (top) and phase (bottom) images of the areas indicated in (B). Schematic representations of possible helix-bundle arrangements are also shown in (top). Poly-**3** and poly-**4** segments are indicated by red and blue lines, respectively.

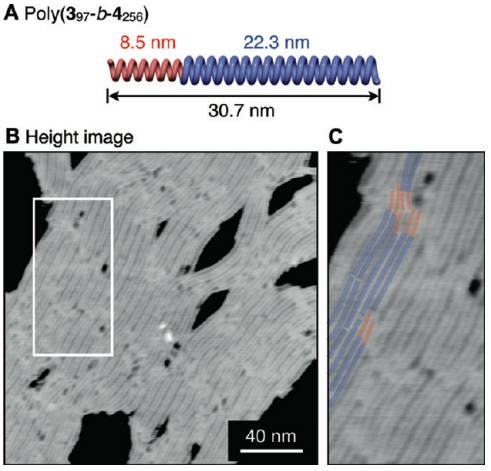

Figure 10. (A) Schematic structure of poly($\mathbf{3}_{97}$-*b*-$\mathbf{4}_{256}$). (B) AFM height image of 2D self-assembled poly($\mathbf{3}_{97}$-*b*-$\mathbf{4}_{256}$) on HOPG prepared in the same manner as in Figure 9. (C) Zoomed image of the area indicated in (B). Schematic representations of possible helix-bundle arrangements are also shown. Poly-**3** and poly-**4** segments are indicated by red and blue lines, respectively.

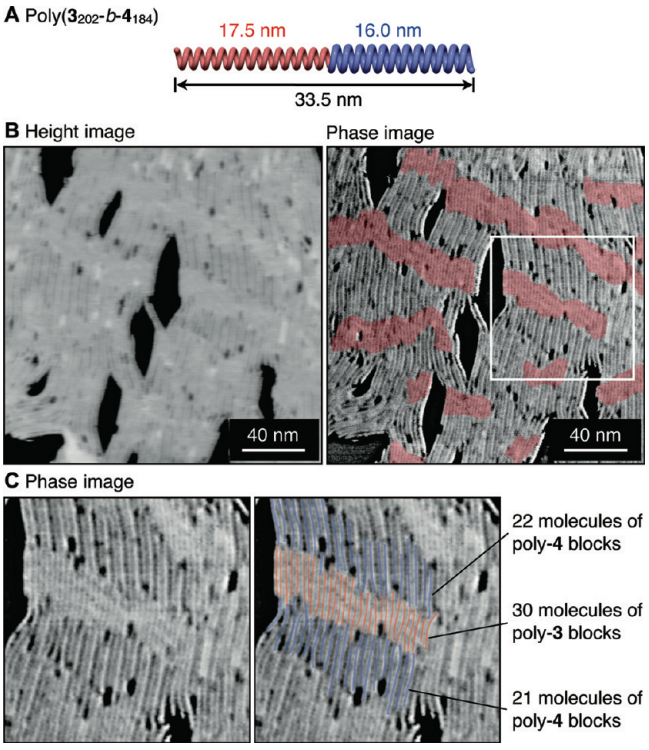

Figure 11. (A) Schematic structure of poly($\mathbf{3}_{202}$-*b*-$\mathbf{4}_{184}$). (B) AFM height (left) and phase (right) images of 2D self-assembled poly($\mathbf{3}_{202}$-*b*-$\mathbf{4}_{184}$) on HOPG prepared in the same manner as in Figure 9. Poly-**3** blocks are indicated by red (right). (C) Zoomed image of the area indicated in (B). Schematic representations of possible helix-bundle arrangements are also shown (right). Poly-**3** and poly-**4** segments are indicated by red and blue lines, respectively.

experimental procedure is described below. The as-prepared poly-**3** ([**3**]/[**2**] = 100) (73.0 mg) dissolved in THF containing 0.1 wt % TBAB was SEC fractionated. After evaporation of the solvent, the fractionated polymer was dissolved in a small amount of THF, the solution was precipitated in a large amount of methanol, and the precipitate was then collected by filtration to remove TBAB. After this procedure was repeated three times, the left-handed helical poly-$\mathbf{3}_{107}(-)$ was obtained (40.9 mg, 56%). In the same way, the left-handed helical poly-$\mathbf{3}_{97}(-)$ and poly-$\mathbf{3}_{202}(-)$ were obtained by SEC fractionation of the as-prepared poly-**3**s ([**3**]/[**2**] = 60 and 120, respectively).

Spectroscopic data of poly-$\mathbf{3}_{107}(-)$: IR (KBr, cm^{-1}): 3280 (ν_{N-H}), 1743 ($\nu_{C=O}$ ester), 1633 (amide I), 1534 (amide II). ^1H NMR ($CDCl_3$, 55 °C, 500 MHz): δ 0.83 (broad, CH_3, 3H), 1.26 (broad, CH_2, 6H), 1.53 (broad, CH_3 and CH_2, 5H), 4.11 (broad, CH_2, 2H), 4.50 (broad, CH, 1H), 4.8−7.7 (broad, aromatic, 4H), 7.9−8.9 (broad, NH, 1H). SEC-MALS: M_n = 3.23×10^4, M_w/M_n = 1.06; $[\alpha]_D^{25}$ −2228 (*c* 0.1, chloroform). Anal. Calcd (%) for $(C_{17}H_{22}N_2O_3)_{107}$: C, 67.53; H, 7.33; N, 9.26. Found: C, 67.77; H, 7.20; N, 9.15.

Spectroscopic data of poly-$\mathbf{3}_{97}(-)$: IR (KBr, cm^{-1}): 3277 (ν_{N-H}), 1742 ($\nu_{C=O}$ ester), 1634 (amide I), 1536 (amide II). ^1H NMR ($CDCl_3$, 55 °C, 500 MHz): δ 0.82 (broad, CH_3, 3H), 1.25 (broad, CH_2, 6H), 1.52 (broad, CH_3 and CH_2, 5H), 4.11 (broad, CH_2, 2H), 4.49 (broad, CH, 1H), 4.8−7.7 (broad, aromatic, 4H), 7.9−8.9 (broad, NH, 1H). SEC-MALS: M_n = 2.95×10^4, M_w/M_n = 1.01; $[\alpha]_D^{25}$ −2106 (*c* 0.1, chloroform). Anal. Calcd (%) for $(C_{17}H_{22}N_2O_3)_{97}$: C, 67.53; H, 7.33; N, 9.26. Found: C, 67.32; H, 7.09; N, 9.05.

Spectroscopic data of poly-$\mathbf{3}_{202}(-)$: IR (KBr, cm^{-1}): 3278 (ν_{N-H}), 1740 ($\nu_{C=O}$ ester), 1633 (amide I), 1537 (amide II). ^1H NMR ($CDCl_3$, 55 °C, 500 MHz): δ 0.81 (broad, CH_3, 3H), 1.25 (broad, CH_2, 6H), 1.51 (broad, CH_3 and CH_2, 5H), 4.11 (broad, CH_2, 2H), 4.49 (broad, CH, 1H), 4.8−7.7 (broad, aromatic, 4H), 7.9−8.9 (broad, NH, 1H). SEC-MALS: M_n = 6.09×10^4, M_w/M_n = 1.01; $[\alpha]_D^{25}$ −2182 (*c* 0.1, chloroform). Anal. Calcd (%) for $(C_{17}H_{22}N_2O_3)_{202}$: C, 67.53; H, 7.33; N, 9.26. Found: C, 67.65; H, 7.14; N, 9.12.

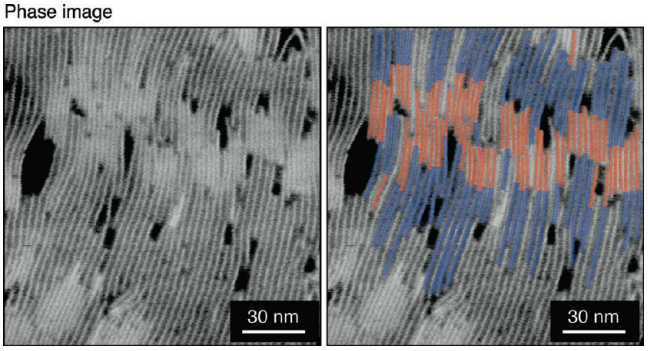

Figure 12. AFM phase images of poly($\mathbf{3}_{202}$-*b*-$\mathbf{4}_{184}$) obtained after further SEC fractionation on HOPG. Poly-**3** and poly-**4** blocks are indicated by red and blue lines, respectively (right).

Block Copolymerization. The block copolymers were prepared in a dry glass ampule under a dry nitrogen atmosphere in dry THF. A typical experimental procedure is described below (Scheme 2). Poly-$\mathbf{3}_{107}(-)$ (9.85 mg) and monomer **4** (13.7 mg, 33.0 mmol) ([**4**]/[**3**] = 1) were placed in a dry ampule, which was then evacuated on a vacuum line and flushed with dry nitrogen. After this evacuation−flush procedure had been repeated three times, a three-way stopcock was attached to the ampule, and dry THF (0.17 mL) was added by a syringe. The mixture solution was then stirred under a dry nitrogen atmosphere and heated to 55 °C. After 30 h, the resulting copolymer (poly($\mathbf{3}_{107}$-*b*-$\mathbf{4}_{92}$)) was precipitated in a large amount of methanol, collected by centrifugation, and dried *in vacuo* at room temperature overnight (23.6 mg, 100% yield). The obtained copolymer was purified by SEC fractionation using THF containing 0.1 wt % TBAB as the eluent. After purification by reprecipitation from chloroform to methanol, the poly($\mathbf{3}_{107}$-*b*-$\mathbf{4}_{92}$) was obtained (18.8 mg, 80% yield).

Spectroscopic data of poly($\mathbf{3}_{107}$-*b*-$\mathbf{4}_{92}$): IR (KBr, cm^{-1}): 3273 (ν_{N-H}), 1747 ($\nu_{C=O}$ ester), 1633 (amide I), 1537 (amide II). ^1H NMR ($CDCl_3$, 55 °C, 500 MHz): δ 0.88 (broad, CH_3), 1.28 (broad, CH_2), 1.52 (broad, CH_3 and CH_2), 4.08 (broad, CH_2), 4.50 (broad, CH), 4.8−7.7 (broad, aromatic), 7.9−9.0 (broad, NH). SEC-MALS: M_n = 7.02×10^4, M_w/M_n = 1.07; $[\alpha]_D^{25}$ −1946 (*c* 0.1, chloroform). Anal. Calcd (%) for $(C_{17}H_{22}N_2O_3)_{107}$-$(C_{25}H_{38}N_2O_3)_{92}$: C, 70.18; H, 8.36; N, 7.91. Found: C, 69.78; H, 8.27; N, 8.24.

In the same way, poly($\mathbf{3}_{97}$-*b*-$\mathbf{4}_{256}$) ([**4**]/[**3**] = 2) and poly($\mathbf{3}_{202}$-*b*-$\mathbf{4}_{184}$) ([**4**]/[**3**] = 1/2) were prepared by the copolymerization of **4** with poly-$\mathbf{3}_{97}(-)$ and poly-$\mathbf{3}_{256}(-)$ as the initiators in THF at 55 °C for 30 h, followed by SEC fractionation and reprecipitation in 70 and 75% yield, respectively.

Spectroscopic data of poly($\mathbf{3}_{97}$-*b*-$\mathbf{4}_{256}$): IR (KBr, cm^{-1}): 3277 (ν_{N-H}), 1747 ($\nu_{C=O}$ ester), 1633 (amide I), 1537 (amide II). ^1H NMR ($CDCl_3$, 55 °C, 500 MHz): δ 0.82 (broad, CH_3), 1.28 (broad, CH_2), 1.52 (broad, CH_3 and CH_2), 4.08 (broad, CH_2), 4.48 (broad, CH), 4.8−7.7 (broad, aromatic), 7.9−9.0 (broad, NH). SEC-MALS: M_n = 1.36×10^5, M_w/M_n = 1.05; $[\alpha]_D^{25}$ −1806 (*c* 0.1, chloroform). Anal. Calcd (%) for $(C_{17}H_{22}N_2O_3)_{97}$-$(C_{25}H_{38}N_2O_3)_{256}$: C, 71.37; H, 8.83; N, 7.30. Found: C, 70.86; H, 8.78; N, 7.00.

Spectroscopic data of poly($\mathbf{3}_{202}$-*b*-$\mathbf{4}_{184}$): IR (KBr, cm^{-1}): 3277 (ν_{N-H}), 1746 ($\nu_{C=O}$ ester), 1634 (amide I), 1538 (amide II). ^1H NMR ($CDCl_3$, 55 °C, 500 MHz): δ 0.87 (broad, CH_3), 1.27 (broad, CH_2), 1.52 (broad, CH_3 and CH_2), 4.08 (broad, CH_2), 4.46 (broad, CH), 4.8−7.7 (broad, aromatic), 7.9−8.9 (broad, NH). SEC-MALS: M_n = 1.37×10^5, M_w/M_n = 1.07; $[\alpha]_D^{25}$ −1887

(*c* 0.1, chloroform). Anal. Calcd (%) for $(C_{17}H_{22}N_2O_3)_{202}$-$(C_{25}H_{38}N_2O_3)_{184}$: C, 70.25; H, 8.39; N, 7.87. Found: C, 69.73; H, 8.55; N, 8.15.

SEC-MALS Measurements. The SEC-MALS measurements were carried out with THF containing 0.1 wt % TBAB used as the eluent at the flow rate of 0.5 mL/min. A standard polystyrene (M_w = 30 500 (Polymer Laboratories, Shropshire, U.K.)) was used to calculate the device constants, such as the interdetector delay, interdetector band broadening, and light scattering detector normalization. The macroinitiator polymers and block copolymers were completely dissolved in the eluent at the concentration of 0.1−0.2% (w/v) under gentle stirring for 1−2 h before injection. The evaluations of the molecular weights were accomplished using ASTRA V software (version 5.1.3.0). The refractive index increment (d*n*/d*c*) values of poly(**3**-*b*-**4**)s in the eluent used for the evaluations were calculated based on the corresponding d*n*/d*c* values of the homopolymers (0.1560 mL/g for poly-**3** and 0.1287 mL/g for poly-**4**), on the assumption that the d*n*/d*c* values were independent of the molecular weight and can be calculated using the equation $(dn/dc) = w_1(dn/dc)_1 + w_2(dn/dc)_2$),[19] where w_1 and w_2 are the weight fraction of the poly-**3** and poly-**4** blocks and $(dn/dc)_1$ and $(dn/dc)_2$ are the refractive index increment of poly-**3** and poly-**4** in the eluent, respectively.

AFM Measurements. Stock solutions of poly($\mathbf{3}_{97}$-*b*-$\mathbf{4}_{256}$), poly($\mathbf{3}_{107}$-*b*-$\mathbf{4}_{92}$), and poly($\mathbf{3}_{202}$-*b*-$\mathbf{4}_{184}$) in dry THF or chloroform (0.02 or 0.005 mg/mL) were prepared. Samples for the AFM measurements were prepared by casting 40 μL aliquots of the stock solutions of the block copolymers. The casting was done at room temperature on freshly cleaved HOPG under THF or chloroform vapor atmospheres. After the polymers had been deposited on the HOPG, the HOPG substrates were further exposed to THF or chloroform vapors for 12 h, and then the substrates were dried under vacuum for 12 h according to the reported procedure.[8] The organic solvent vapors were prepared by putting 1 mL of THF or chloroform into a 2 mL flask that was inside a 50 mL flask, and the HOPG substrates were then placed in the 50 mL flask. The typical settings of the AFM for the high-magnification observations were as follows: amplitude 1.0−1.5 V; set point 0.9−1.4 V; scan rate 2.5 Hz. The Nanoscope image processing software was used for the image analysis.

Molecular Modeling and Calculations. The molecular modeling and molecular mechanics (MM) calculations were conducted with the Compass force field,[20] as contained in the MS Modeling software (version 4.4, Accelrys, San Diego, CA) operated using a PC running under Windows XP. The polymer models (50 repeating monomer units) of poly-**3** and poly-**4** were constructed using the Polymer Builder module in the MS Modeling software with the suitable side-chain conformations. The starting main-chain geometrical parameters, such as the bond lengths, the bond angles, and the internal rotation angles, were defined as a 15 unit/4 turn (15/4) helix on the basis of the left-handed helical structure of the poly(phenyl isocyanide) bearing L-alanine pendants with an *n*-decyl chain determined by X-ray analysis.[8] The geometric parameters of the main chain were fixed during the following force-field optimization. The dielectric constant was set to 1.0. The geometry optimizations were carried out without any cutoff by the smart minimizer in three steps. First, the starting conformations were subject to the steepest decent optimization to eliminate the worse steric conflicts. Second, subsequent optimization until the convergence using a conjugate gradient algorithm was performed. The fully optimized polymer models were obtained by the further energy minimization using the Newton method with the 0.1 kcal/mol/Å convergence criterion; the bond lengths, the bond angles, and the internal rotation angles of the main chains were −67.1°, 106.8°, and 1.46 Å, respectively (Figure 1B).

Acknowledgment. We are deeply grateful to Professor K. Onitsuka (Osaka University) for his generous supply of the Pt−Pd catalyst. This work was supported in part by Grant-in-Aid for Scientific Research (S) from the Japan Society for the Promotion of Science (JSPS), Japan Science and Technology Agency (JST), and the Global COE Program "Elucidation and Design of Materials and Molecular Functions" of the Ministry of Education, Culture, Sports, Science, and Technology, Japan. Z.-Q.W. thanks the JSPS for a postdoctoral fellowship for foreign researchers (No. P06350). K.N. expresses his thanks for a JSPS Research Fellowship for Young Scientists (No. 6683).

Supporting Information Available: AFM images of 2D self-assembled homopolymers of poly-**3** and poly-**4** (an equimolar mixture) on HOPG and SEC chromatograms of poly-**3**s and poly(**3**-*b*-**4**)s before and after SEC fractionation (PDF). This material is available free of charge via the Internet at http://pubs.acs.org.

References and Notes

(1) (a) Chen, J. T.; Thomas, E. L.; Ober, C. K.; Mao, G.-p. *Science* **1996**, *273*, 343–346. (b) Stupp, S. I.; LeBonheur, V.; Walker, K.; Li, L. S.; Huggins, K. E.; Keser, M.; Amstutz, A. *Science* **1997**, *276*, 384–389. (c) Cornelissen, J. J. L. M.; Fischer, M.; Sommerdijk, N. A. J. M.; Nolte, R. J. M. *Science* **1998**, *280*, 1427–1430. (d) Jenekhe, S. A.; Chen, X. L. *Science* **1999**, *283*, 372–375. (e) Zubarev, E. R.; Pralle, M. U.; Sone, E. D.; Stupp, S. I. *J. Am. Chem. Soc.* **2001**, *123*, 4105–4106. (f) Kim, K. T.; Park, C.; Kim, C.; Winnik, M. A.; Manners, I. *Chem. Commun.* **2006**, 1372–1374. For recent reviews: (g) Lee, M.; Cho, B.-K.; Zin, W.-C. *Chem. Rev.* **2001**, *101*, 3869–3892. (h) Cornelissen, J. J. L. M.; Rowan, A. E.; Nolte, R. J. M.; Sommerdijk, N. A. J. M. *Chem. Rev.* **2001**, *101*, 4039–4070. (i) Klok, H.-A.; Lecommandoux, S. *Adv. Mater.* **2001**, *13*, 1217–1229. (j) Olsen, B. D.; Segalman, R. A. *Mater. Sci. Eng., R* **2008**, *62*, 37–66.

(2) (a) Scherf, U.; Gutacker, A.; Koenen, N. *Acc. Chem. Res.* **2008**, *41*, 1086–1097. (b) Scherf, U.; Adamczyk, S.; Gutacker, A.; Koenen, N. *Macromol. Rapid Commun.* **2009**, *30*, 1059–1065.

(3) Kros, A.; Jesse, W.; Metselaar, G. A.; Cornelissen, J. J. L. M. *Angew. Chem., Int. Ed.* **2005**, *44*, 4349–4352.

(4) (a) Cornelissen, J. J. L. M.; Donners, J. J. J. M.; de Gelder, R.; Graswinckel, W. S.; Metselaar, G. A.; Rowan, A. E.; Sommerdijk, N. A. J. M.; Nolte, R. J. M. *Science* **2001**, *293*, 676–680. (b) Cornelissen, J. J. L. M.; Sommerdijk, N. A. J. M.; Nolte, R. J. M. *Macromol. Chem. Phys.* **2002**, *203*, 1625–1630. (c) Samorí, P.; Ecker, C.; Gössl, I.; de Witte, P. A. J.; Cornelissen, J. J. L. M.; Metselaar, G. A.; Otten, M. B. J.; Rowan, A. E.; Nolte, R. J. M.; Rabe, J. P. *Macromolecules* **2002**, *35*, 5290–5294. (d) Cornelissen, J. J. L. M.; Graswinckel, W. S.; Rowan, A. E.; Sommerdijk, N. A. J. M.; Nolte, R. J. M. *J. Polym. Sci., Part A: Polym. Chem.* **2003**, *41*, 1725–1736. (e) Metselaar, G. A.; Cornelissen, J. J. L. M.; Rowan, A. E.; Nolte, R. J. M. *Angew. Chem., Int. Ed.* **2005**, *44*, 1990–1993. (f) Metselaar, G. A.; Adams, P. J. H. M.; Nolte, R. J. M.; Cornelissen, J. J. L. M.; Rowan, A. E. *Chem.—Eur. J.* **2007**, *13*, 950–960. (g) Metselaar, G. A.; Wezenberg, S. J.; Cornelissen, J. J. L. M.; Nolte, R. J. M.; Rowan, A. E. *J. Polym. Sci., Part A: Polym. Chem.* **2007**, *45*, 981–988. For recent reviews on helical polyisocyanides, see ref 1h and (h) Takahashi, S.; Onitsuka, K.; Takei, F. *Proc. Jpn. Acad., Ser. B* **1998**, *74*, 25–30. (i) Suginome, M.; Ito, Y. *Adv. Polym. Sci.* **2004**, *171*, 77–136. (j) Amabilino, D. B.; Serrano, J.-L.; Sierra, T.; Veciana, J. *J. Polym. Sci., Part A: Polym. Chem.* **2006**, *44*, 3161–3174.

(5) (a) Pauling, L.; Corey, R. B. *Proc. Natl. Acad. Sci. U.S.A.* **1951**, *37*, 241–250. (b) Doty, P.; Lundberg, R. D. *J. Am. Chem. Soc.* **1956**, *78*, 4810–4812. (c) Doty, P.; Lundberg, R. D. *J. Am. Chem. Soc.* **1957**, *79*, 2338–2339. (d) Lundberg, R. D.; Doty, P. *J. Am. Chem. Soc.* **1957**, *79*, 3961–3972.

(6) (a) Bellomo, E. G.; Wyrsta, M. D.; Pakstis, L.; Pochan, D. J.; Deming, T. J. *Nature Mater.* **2004**, *3*, 244–248. (b) Kong, X.; Jenekhe, S. A. *Macromolecules* **2004**, *37*, 8180–8183. (c) Park, S.; Lim, J.-H.; Chung, S.-W.; Mirkin, C. A. *Science* **2004**, *303*, 348–351.

(7) (a) Onitsuka, K.; Joh, T.; Takahashi, S. *Bull. Chem. Soc. Jpn.* **1992**, *65*, 1179–1181. (b) Onitsuka, K.; Joh, T.; Takahashi, S. *Angew. Chem., Int. Ed. Engl.* **1992**, *31*, 851–852. (c) Onitsuka, K.; Joh, T.; Takahashi, S. *Chem.—Eur. J.* **2000**, *6*, 983–993. (d) Takei, F.; Hayashi, H.; Onitsuka, K.; Kobayashi, N.; Takahashi, S. *Angew. Chem., Int. Ed.* **2001**, *40*, 4092–4094.

(8) Onouchi, H.; Okoshi, K.; Kajitani, T.; Sakurai, S.-i.; Nagai, K.; Kumaki, J.; Onitsuka, K.; Yashima, E. *J. Am. Chem. Soc.* **2008**, *130*, 229–236.

(9) The persistence length of the polymer prepared by the polymerization of the same monomer with an achiral $NiCl_2$ catalyst, whose helical sense (right- or left-handed helix) could be controlled by the polymerization solvent and temperature,[9a,b] was determined to be 220 nm,[9c] although it does not have a perfect one-handed helical structure. To our knowledge, this value is the highest among all the synthetic helical polymers prepared so far. (a) Kajitani, T.; Okoshi, K.; Sakurai, S.-i.; Kumaki, J.; Yashima, E. *J. Am. Chem. Soc.* **2006**, *128*, 708–709. (b) Kajitani, T.; Okoshi, K.; Yashima, E. *Macromolecules* **2008**, *41*, 1601–1611. (c) Okoshi, K.; Nagai, K.; Kajitani, T.; Sakurai, S.-i.; Yashima, E. *Macromolecules* **2008**, *41*, 7752–7754.

(10) Wu, Z.-Q.; Nagai, K.; Banno, M.; Okoshi, K.; Onitsuka, K.; Yashima, E. *J. Am. Chem. Soc.* **2009**, *131*, 6708–6718.

(11) The helical sense and helical sense excess (> 99%) of poly-**3**s were determined by a comparison of the sign and intensity of the Cotton effects at 364 nm with those of an analogous L-alanine-bound polyisocyanide (poly-**1**) whose helical sense and helical sense excess had been determined by direct AFM measurements.[8]

(12) Poly($\mathbf{3}_{202}$-*b*-$\mathbf{4}_{184}$) showed a nematic-like LC phase probably because the sample contained a small amount of the macroinitiator (poly-$\mathbf{3}_{202}$(−)) (see text).

(13) This method is very useful for constructing highly ordered 2D helix bundles for helical polyacetylenes[14] and polyisocyanides[8,9a,10] on HOPG, and their helical structures were visualized by AFM.

(14) (a) Sakurai, S.-i.; Okoshi, K.; Kumaki, J.; Yashima, E. *Angew. Chem., Int. Ed.* **2006**, *45*, 1245–1248. (b) Sakurai, S.-i.; Okoshi, K.; Kumaki, J.; Yashima, E. *J. Am. Chem. Soc.* **2006**, *128*, 5650–5651. (c) Sakurai, S.-i.; Ohsawa, S.; Nagai, K.; Okoshi, K.; Kumaki, J.; Yashima, E. *Angew. Chem., Int. Ed.* **2007**, *46*, 7605–7608. For recent reveiws, see: (d) Yashima, E.; Maeda, K. *Macromolecules* **2008**, *41*, 3–12. (e) Yashima, E.; Maeda, K.; Furusho, Y. *Acc. Chem. Res.* **2008**, 1166–1180. (f) Kumaki, J.; Sakurai, S.-i.; Yashima, E. *Chem. Soc. Rev.* **2009**, *38*, 737–746. (g) Yashima, E.; Maeda, K.; Iida, H.; Furusho, Y.; Nagai, K. *Chem. Rev.* **2009**, *109*, 6102–6211.

(15) For similar AFM observations of the smectic-like layer structures composed of synthetic helical polymers exhibiting smectic LC phases, see: (a) Oka, H.; Suzaki, G.; Edo, S.; Suzuki, A.; Tokita, M.; Watanabe, J. *Macromolecules* **2008**, *41*, 7783–7786. (b) Okoshi, K.; Suzuki, A.; Tokita, M.; Fujiki, M.; Watanabe, J. *Macromolecules* **2009**, *42*, 3443–3447.

(16) For phase-separated lamellar structures composed of conjugated rod−rod or rod−coil−rod block copolymers observed by AFM and TEM, see ref 2 and (a) Hayakawa, T.; Goseki, R.; Kamimoto, M.; Tokita, M.; Watanabe, J.; Liao, Y.; Horiuchi, S. *Org. Lett.* **2006**, *8*, 5453–5456. (b) Zhang, Y.; Tajima, K.; Hirota, K.; Hashimoto, K. *J. Am. Chem. Soc.* **2008**, *130*, 7812–7813. (c) Kim, J.-H.; Rahman, M. S.; Lee, J.-S.; Park, J.-W. *Macromolecules* **2008**, *41*, 3181–3189. (d) Wu, P.-T.; Ren, G.; Li, C.; Mezzenga, R.; Jenekhe, S. A. *Macromolecules* **2009**, *42*, 2317–2320.

(17) An equimolar mixture of the homopolymers of poly-**3** and poly-**4** also self-assembled on the HOPG into small domains composed of 2D helix bundles with different chain-to-chain spacings of 1.8 and 2.6 nm and an almost identical average height of 1.7 nm, although no banded texture could be formed as expected. Quite interestingly, the AFM image of the same sample after 7 days clearly showed domains with different heights similar to those observed for poly-($\mathbf{3}_{107}$-*b*-$\mathbf{4}_{92}$), which also supports the assignments of the block segments of poly($\mathbf{3}_{107}$-*b*-$\mathbf{4}_{92}$) on HOPG (Figure S1).

(18) Possible helical structures of the left-handed helical poly-**3** and poly-**4** (Figure 1B) were calculated on the basis of a 15/4 helical structure of poly-**1** determined by the XRD analyses followed by molecular mechanics calculations (see Experimental Section). The diameters of the cylindrical polyisocyanides slightly increased with an increase in the alkyl chains. However, the average heights of each of the homopolymers (ca. 1.7 nm) estimated by AFM were significantly shorter than the computer-generated molecular diameters of poly-**3** (2.8 nm) and poly-**4** (3.2 nm). The strong interaction of the pendant long alkyl chains with the HOPG surface and a tip-induced deformation of the samples should be taken into consideration for the reduced heights on HOPG.

(19) Bushuk, W.; Benoit, H. *Can. J. Chem.* **1958**, *36*, 1616–1626.

(20) Sun, H. *J. Phys. Chem. B* **1998**, *102*, 7338–7364.